



## Comparison of the three different approaches for damage detection in the part of the composite wind turbine blade

Luczak, M.; Peeters, B.; Szkudlarek, W.; Mevel, L.; Döhler, M.; Ostachowicz, W.; Branner, Kim; Martyniuk, Karolina

*Published in:*  
Proceedings

*Publication date:*  
2009

*Document Version*  
Early version, also known as pre-print

[Link back to DTU Orbit](#)

*Citation (APA):*  
Luczak, M., Peeters, B., Szkudlarek, W., Mevel, L., Döhler, M., Ostachowicz, W., Branner, K., & Martyniuk, K. (2009). Comparison of the three different approaches for damage detection in the part of the composite wind turbine blade. In *Proceedings*

---

### General rights

Copyright and moral rights for the publications made accessible in the public portal are retained by the authors and/or other copyright owners and it is a condition of accessing publications that users recognise and abide by the legal requirements associated with these rights.

- Users may download and print one copy of any publication from the public portal for the purpose of private study or research.
- You may not further distribute the material or use it for any profit-making activity or commercial gain
- You may freely distribute the URL identifying the publication in the public portal

If you believe that this document breaches copyright please contact us providing details, and we will remove access to the work immediately and investigate your claim.

## COVER SHEET

Title: Comparison of the three different approaches for damage detection in the part of the composite wind turbine blade.

Marcin Luczak([marcin.luczak@lmsintl.com](mailto:marcin.luczak@lmsintl.com)), Bart Peeters, Wojciech Szkudlarek, LMS International, Interleuvenlaan 68, B-3001 Heverlee, Belgium,

Laurent Mevel ([laurent.mevel@irisa.fr](mailto:laurent.mevel@irisa.fr)), Michael Döhler, INRIA, Centre Rennes - Bretagne Atlantique, Campus de Beaulieu, F-35042 Rennes, France

Wieslaw Ostachowicz ([wieslaw@imp.gda.pl](mailto:wieslaw@imp.gda.pl)), Institute of Fluid Flow Machinery, Polish Academy of Sciences, ul. Fiszer 14, 80 952 Gdansk, Poland

Karolina Martyniuk ([karm@risoe.dtu.dk](mailto:karm@risoe.dtu.dk)), Kim Branner, Wind Energy Department Risø National Laboratory for Sustainable Energy Technical University of Denmark, DTU Building 118, DK-4000 Roskilde, Denmark <sup>1</sup>

---

Marcin Luczak([marcin.luczak@lmsintl.com](mailto:marcin.luczak@lmsintl.com)), Bart Peeters, Wojciech Szkudlarek, LMS International, Interleuvenlaan 68, B-3001 Heverlee, Belgium,  
Laurent Mevel ([laurent.mevel@irisa.fr](mailto:laurent.mevel@irisa.fr)), Michael Döhler, INRIA, Centre Rennes - Bretagne Atlantique, Campus de Beaulieu, F-35042 Rennes, France  
Wieslaw Ostachowicz ([wieslaw@imp.gda.pl](mailto:wieslaw@imp.gda.pl)), Institute of Fluid Flow Machinery, Polish Academy of Sciences, ul. Fiszer 14, 80 952 Gdansk, Poland  
Karolina Martyniuk ([karm@risoe.dtu.dk](mailto:karm@risoe.dtu.dk)), Kim Branner, Wind Energy Department Risø National Laboratory for Sustainable Energy Technical University of Denmark, DTU Building 118, DK-4000 Roskilde, Denmark

## ABSTRACT

This paper presents a scope and results comparison of three SHM methods applied for the damage detection in the composite material wind turbine blade parts.

All three methods are based on the model identification of the undamaged structure and afterwards, models from a measurement of damaged structure are confronted with the model of the intact structure. The presence of test data variability is accounted to prevent “false alarm” due to the non-identical nature of three nominally equal composite material specimens under investigation (samples A, B and C). For each of these specimens identical damage scenario was introduced but to a different level (severe, intermediate and low).

The first method is statistical model-based damage detection using subspace-based algorithms. It is using output-only time data series from the vibration acceleration measurement. The reference parameter is the modal signature of a state-space model of the studied system, and the tests aim at detecting small deviations in this signature without explicitly computing it. Damage is monitored by reducing time data to covariance data and performing a subspace-based chi-square test. Parameter variation in the signal from nominal and damaged structure allows assessing healthy/not healthy status.

The second method is based on PZT transducers and A0 mode of the Lamb waves propagating in a multilayer composite plate. A piezoelectric actuator generates the Lamb wave. Propagating elastic wave is reflected from both the eventual damage and the boundaries of the plate. A piezoelectric sensor network acquires the response signal. The proposed damage detection algorithm makes use of the assumption that the excitation signal and signals reflected from damage have matching features. If this is true the idea is to search all signals registered for signals reflected from damage and subsequently to compare the features of these signals with the features of the excitation signal. The excitation signal has a finite length and thus can be thought of as surrounded by a virtual time window. This time window can be arbitrarily placed on each of the registered signals resulting in

a certain time shift, which is equivalent to a distance required for the propagating signal to travel from the excitation point to a point P of coordinates x and y (possible damage location) and then back to an appropriate sensors.

In the third method a progressive damage is monitored using polyreference LSCF (also called polymax) to estimate the modal parameters and follow their deviations. For the initial measurement of the intact structure a specimen (each individually) was supported in free-free boundary conditions by means of the elastic cords attached to a plate. An electrodynamic shaker was applied as a source for the excitation. Different excitation signals were applied (pure random, burst random). The response signals of the structure were measured by a set of piezoceramic accelerometers. Time series and FRF functions were acquired. Three nominally identical specimens were tested to obtain an experimental data collection which can be processed to obtain statistical measures.

The statistical assessment of the initial parameters from three intact specimens is presented. The results from detection of the three levels of the same damage using three different approaches are compared and discussed.

## 1. INTRODUCTION

The paper presents the results of the damage detection investigation in the multilayer E-glass wind turbine blade composite material with three SHM methods. The objects of the investigation were three nominally identical plates A, B and C. The nominal dimension were 20×320×320 mm (see Figure 2). Due to non repeatable manufacturing process dimension variability reaches ±0.7%. Damage was introduced into plates by means of four-point bending quasi-static test. Plate A was loaded with the force of 230 kN, plate B 210 kN and place C 220 kN. The scope and results of each method is presented in following sections.

## 2. SUBSPACE-BASED IDENTIFICATION AND DAMAGE DETECTION

### 2.1 Subspace-based Covariance Driven Identification Algorithm

We consider a linear multi-variable output-only system described by a discrete-time state space model:

$$\begin{cases} X_{k+1} = FX_k + V_{k+1} \\ Y_k = HX_k \end{cases} \quad (1)$$

where state X and observed output Y, at each time sample k, have dimensions m and r respectively. The state noise V is assumed to be stationary, unmeasured Gaussian white noise with zero mean. For system identification we construct the Hankel matrix

$$H_{p+1,q} \stackrel{\text{def}}{=} \begin{pmatrix} R_0 & R_1 & \cdots & R_{q-1} \\ R_1 & R_2 & \cdots & R_q \\ \vdots & \vdots & & \vdots \\ R_p & R_{p+1} & \cdots & R_{p+q-1} \end{pmatrix} \stackrel{\text{def}}{=} \text{Hank}(R_i) \quad (2)$$

containing the covariances  $R_i = E(Y_k Y_{k-i}^T)$ , use the well-known factorization property of  $H_{p+1,q}$  into observability and controllability matrix and recover H and F from the observability matrix. The eigenstructure  $(\lambda, \Phi_\lambda)$  of the system (1) and a corresponding modal parameter  $\theta$  are retrieved from

$$\det(F - \lambda I) = 0, (F - \lambda I)\phi_\lambda = 0, \Phi_\lambda \stackrel{\text{def}}{=} H\phi_\lambda, \theta \stackrel{\text{def}}{=} \begin{pmatrix} \Lambda \\ \text{vec } \Phi \end{pmatrix} \quad (3)$$

where  $\Lambda$  is the vector whose elements are the  $\lambda$ 's and  $\Phi$  is the matrix whose columns are the  $\Phi_\lambda$ 's. The natural frequencies and damping values of the system (1) are computed from the  $\lambda$ 's, see also [1].

The outputs  $Y_k$  for each of the plates were measured at 49 points during four passes: at 14 points in the first three passes and at 7 in the 4th pass. The excitation is assumed to be different for each of the four passes due to slight changes in the environmental conditions, but stationary during each pass. Hence the state noise  $V$  in (1) has a different variance for all the four passes and the measurements are normalised with respect to a change in the excitation. A merged matrix  $H_{p+1,q}$  containing measurement information from all the four passes is obtained according to the merging procedure described in [1].

## 2.2 Damage Detection

For our subspace-based damage detection method a statistical comparison is made by defining a decision variable evaluating the system state [2]. This decision variable is an asymptotically centered Gaussian variable when the system is near the reference/healthy state ( $\theta = \theta_0$ ) and non-centered in case of a change in modal parameters ( $\theta \neq \theta_0$ ), which can be determined with an appropriate  $\chi^2$  test. We compute our decision variable  $\zeta_n$  as the residual:

$$\zeta_n \stackrel{\text{def}}{=} \sqrt{n} \text{vec}(S^T \hat{H}_{p+1,q}) \quad \text{with} \quad \hat{H}_{p+1,q} = \text{Hank}(\hat{R}_i), \quad \hat{R}_i = \frac{1}{n} \sum_{k=1}^n Y_k Y_{k-i}^T \quad (4)$$

where  $n$  is the sample length,  $S$  is the left kernel of the Hankel matrix at the reference state and  $\hat{H}_{p+1,q}$  is the Hankel matrix at the actual state. With the residual covariance  $\Sigma$  at the reference state, the global  $\chi^2$  test statistics built on the residual boils down to [2, 3]

$$\chi_n^2 = \zeta_n^T \Sigma^{-1} \zeta_n \quad (5)$$

As there are three references in our example (plates A, B and C in intact state, resp. Hankel matrices  $\hat{H}_{p+1,q}^{(A)}$ ,  $\hat{H}_{p+1,q}^{(B)}$ ,  $\hat{H}_{p+1,q}^{(C)}$ ), we create a residual  $\zeta_n$  robust to all the plates by computing the left kernel  $S$  on the juxtaposed matrix  $(\hat{H}_{p+1,q}^{(A)} \hat{H}_{p+1,q}^{(B)} \hat{H}_{p+1,q}^{(C)})$ , inspired by the temperature change rejection approach in [3]. The damage detection is then done by computing the appropriate  $\chi^2$  test (5) and comparing it to a threshold.

### 2.3 Numerical Results

With the subspace-based identification algorithm of Section 2.1 we computed the natural frequencies ( $f$ ) and damping coefficients ( $d$ ) of the three plates in intact and damaged state. Nine modes were recovered (see Table I).

For the damage detection test of Section 2.2 we cut the signals in 12 parts and computed the left kernel  $S$  for the decision variable  $\zeta_n$  on three Hankel matrices – one for each plate – containing healthy data of the first part only. To test the robustness the  $\chi^2$  values (5) were calculated on all the parts of the signals from the intact and damaged state separately and finally averaged over all 12 parts to get a meaningful average, see Figure 1.

TABLE I. NATURAL FREQUENCIES AND DAMPING COEFFICIENTS.

Mode	A intact		A damaged		B intact		B damaged		C intact		C damaged	
	$f$ (Hz)	$d$ (%)	$f$ (Hz)	$d$ (%)	$f$ (Hz)	$d$ (%)	$f$ (Hz)	$d$ (%)	$f$ (Hz)	$d$ (%)	$f$ (Hz)	$d$ (%)
1	350	2.2	257	1.1	357	2.1	358	1.0	359	1.7	359	2.4
2	559	2.5	387	1.1	564	1.5	538	1.0	554	3.5	545	3.7
3	818	3.3	528	2.1	788	2.6	784	0.6	784	3.3	835	3.0
4	917	1.8	654	1.5	919	1.9	957	1.4	929	2.7	928	2.4
5	1081	1.1	729	1.1	1102	3.3	1123	0.9	1097	1.9	1106	1.6
6	1246	5.7	-	-	1292	5.8	1295	3.8	1270	5.0	1242	2.5
7	1472	1.5	874	1.3	1536	2.4	1515	1.9	1506	2.4	1554	2.5
8	1849	1.3	1108	1.3	1846	2.5	1844	1.1	1850	2.1	1835	1.3
9	1934	2.5	1273	1.4	1962	3.6	1927	1.7	1946	1.7	1891	1.9

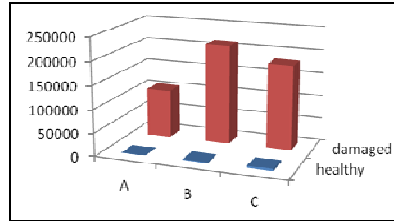
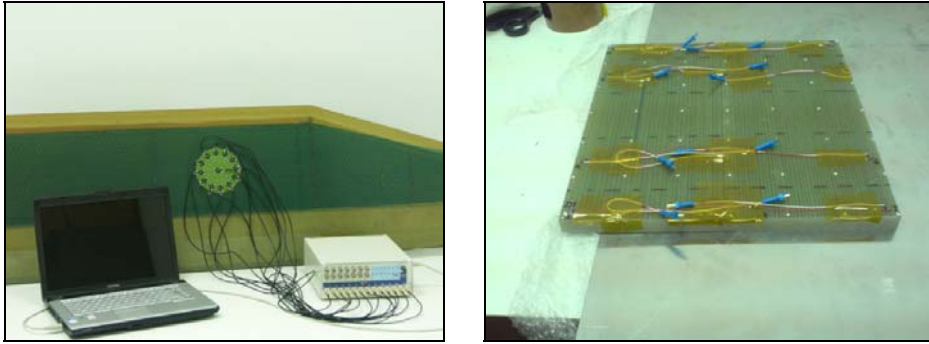


Figure 1.  $\chi^2$  damage detection test on intact and damaged plates.

### 3. ELASTIC WAVE PROPAGATION METHOD

This damage detection method is based on elastic wave propagation method that is recently widely used for damage detection and localisation problems. Mentioned method utilises fact that discontinuities existing in structures cause local changes in material properties that disturb elastic wave propagation. In comparison to other well known non-destructive testing methods presented method is very sensitive to discontinuities because of the use of high frequency signals. Described non-destructive method can be used both for isotropic as well composite structures.

Measurement set-up (see Figure 2) consists of electronic equipment for signals generation and acquisition, piezoelectric transducers as active elements for elastic wave generation and portable PC for signals storage and processing. Distributed piezoelectric transducers network have been placed on composite sample from wind turbine blade (see Figure 2). Piezoelectric network consists of twelve Noliac CMAP06 transducers attached to the composite part using cyanoacrylate glue. Excitation has been applied to each transducer from configuration while registration has been realised in the rest transducers. In result 144 signals have been obtained for intact plate and the same number of signals has been obtained from measurement for damaged specimen.



**Figure 2. Electronic system for elastic waves generation/acquisition (left) and composite part of wind turbine blade equipped with piezoelectric (right).**

Algorithm used for damage detection divides surface to be monitored into a mesh of points  $P_i=(x_i, y_i)$ . Points separation was chosen to be constant and equal to

$$s = A c_g \frac{N}{f_c} \quad (6)$$

where  $c_g$  – Lamb wave group velocity,  $N$  – number of sine cycles in excitation,  $f_c$  – excitation central frequency,  $A$  – ratio to be chosen. Therefore  $s$  is strictly connected with excited wave. In order to project registered time signals to monitored surface signals differences were calculated  $B_{jk}(t)$  – signals from intact sample  $B_{jk}^r(t)$  were subtracted from signals for potentially damaged sample  $B_{jk}^d(t)$

$$B_{jk}(t) = B_{jk}^d(t) - B_{jk}^r(t), \quad (7)$$

where  $i, j$  denote generating and receiving transducer number, respectively.

Next, distances between wave generating transducer to mesh point  $|T_j P_i|$  and from this point to wave receiving transducer  $|P_i R_k|$  were calculated and used to cut out a part of a signal registered in  $R_k$  with generation in  $T_j$ . The cut out part has a length of  $l=s/c_g$  and is centred in

$$t_{jk}^i = \frac{|T_j P_i| + |P_i R_k|}{c_g}. \quad (8)$$

Let's denote this part of the signal as  $F_n$ , this signal is discrete so the index takes values  $n=1,2,\dots,N$ ,  $N$  depends on the length  $l$ . The signals are mapped into point  $P_i$  by summing signal power (squared signal) from all the  $T_j$  and  $R_k$  pairs:

$$M(P_i) = \sum_{j=1}^J \sum_{k=1}^K \sum_{n=1}^N F_n^2. \quad (9)$$

This procedure is repeated for all point  $P_i$  in considered mesh. Such signal processing approach causes that the  $M(P_i)$  lies on an ellipsis which loci are  $T_j$  and  $R_k$  [4, 5].

In the conducted experiment  $A=0.1$  was chosen. It gave a good balance between computational speed and resolution of the mapping. Results for two considered frequencies (100 and 110 kHz) are depicted on Figure 3. Obtained results were normalised to the maximum value. Conducted mapping procedure indicated that the greatest differences between damaged and intact sample are in its lower half (see Figure 3). This suggests that damage could occur in this area. However it should be underlined that the difference could be also a result of transducer debonding caused by bending procedure. In order to ensure this is not the reason a transducer self-testing procedure ought to be incorporated in the detection procedure.

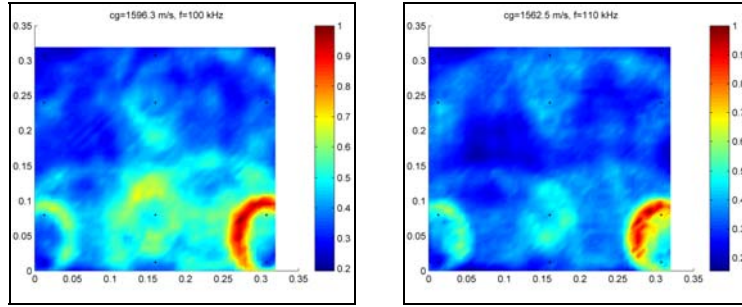


Figure 3. Results of damage detection using Lamb wave propagation for two central frequencies 100 (left) and 110 kHz (right).

#### 4. POLYREFERENCE LSCF (PolyMAX) METHOD

The Polyreference LSCF (PolyMAX) analysis method is based on Input/Output data in Frequency Domain (compare with Subspace method based on Output data in Time Domain). This method is used for estimation and comparison of the modal models identified for intact (reference) and damaged structure. In the LMS PolyMAX method [6] following so-called right matrix-fraction model is assumed to represent the measured FRF's:

$$[H(\omega)] = \sum_{r=0}^p z^r [\beta_r] \left( \sum_{r=0}^p z^r [\alpha_r] \right)^{-1} \quad (10)$$

where  $[H(\omega)] \in C^{ixm}$  is the matrix containing the FRF's between all  $m$  inputs and all  $l$  outputs;  $[\beta_r] \in R^{ixm}$  the numerator matrix of polynomial are coefficients; the



denominator matrix polynomial coefficients  $[\alpha_r] \in R^{mxm}$ . It should be noted that the so-called Z-domain model was used in Eq. 10. Once the denominator coefficients  $[\alpha_r]$  and  $[\beta_r]$  are determined (Least-Squares solution of Eq. 10), the poles and modal participation factors are retrieved as the eigenvalues and eigenvectors of their companion matrix.

Data analysed with subspace based method described in Section 2 and PolyMAX was acquired from the same experimental setup build with LMS acquisition hardware and software. Main difference is that subspace algorithm works on output-only time domain signals while PolyMAX uses the frequency domain input/output FRFs. Number of natural frequencies and mode shapes identified from those two data sets are identical for the intact plates. In frequency domain analysis corresponding natural frequencies are slightly shifted towards higher values due to the influence of the shaker (see Table I and II). This phenomenon is described in details in the [7]. Number of identical experiments followed by modal parameter estimation revealed existence of the scatter of identified frequencies values within consecutive tests of the same plate and in between plates A, B and C as well. Modal model parameters range caused by test data variability was statistically assessed on the dimensionless frequencies values and is presented on the Figure 4.

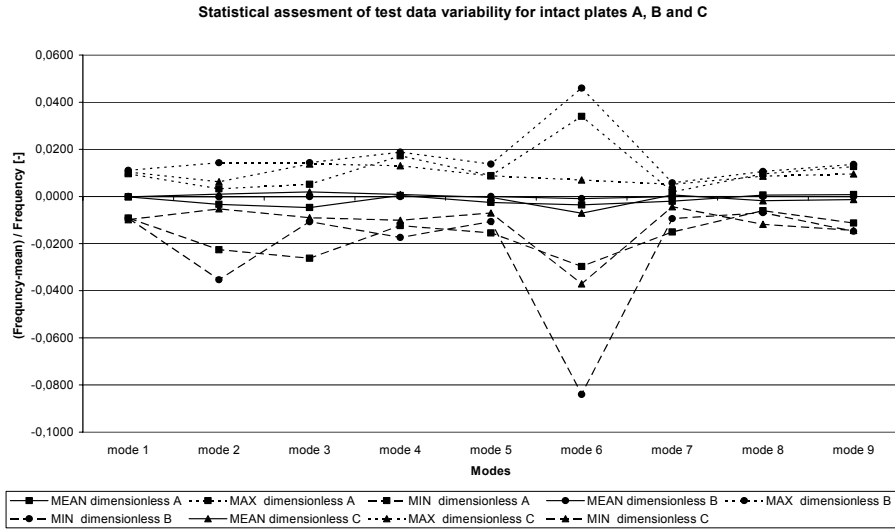
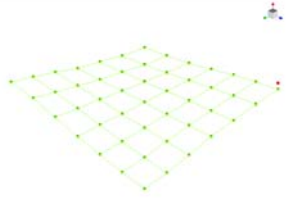
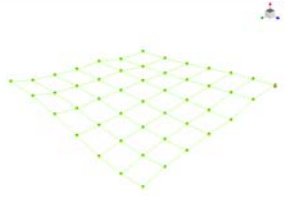


Figure 4. Test data variability leading to frequency values scatter.

TABLE II. MODE SHAPE AND NATURAL FREQUENCIES.

Intact sample	Damaged sample
 <p>First mode 378 Hz</p>	 <p>First mode 270 Hz</p>

Highest scatter observed for the sixth mode values is caused by relatively weak excitation of this mode. Damage was successfully detected in all three specimens. Example for plate A is presented in Table II. Next to the decrease of natural frequency values caused by stiffness degradation due to delamination, fiber cracks and fiber-matrix debonding in all three plates appeared new modes. In the plate A with the largest damage three new modes were identified, in plate B there are two damage related modes and in plate C one mode.

## 5. CONCLUSIONS AND FURTHER RESEARCH

The comparison of three different damage detection methods in presence of test data variability for the E-glass composite material part of wind turbine blade was presented. All three methods proved their adequacy in detecting different levels of the damage. However the unexpected observation of increased natural frequency of some modes require more in-depth investigation. Therefore the scope of further research will focus on the precise identification of damage level and location by means of ultrasonic methods and radiography. Modal data will be processed with the application of the modal filter which is reported in many scientific papers as an indicator in order to differentiate between damage and intact state.

## 6. ACKNOWLEDGEMENTS

The authors gratefully acknowledge support for this research project “UNVICO-2” provided by the 6th EU FP Marie Curie Fellowships and T. Wandowski and P. Malinowski from IFFM PASci for their contribution.

## REFERENCES

1. Mevel, L., M. Basseville, A. Benveniste, and M. Goursat. 2002. “Merging sensor data from multiple measurement setups for nonstationary subspace-based modal analysis,” *J. Sound Vib.*, 249(4):719-741.
2. Mevel, L., M. Goursat, and M. Basseville. 2003. “Stochastic subspace-based structural identification and damage detection and localization - Application to the Z24 bridge benchmark,” *Mech. Syst. Signal Pr., Special issue on COST F3 Benchmarks*, 17(1):143-151.
3. Balmès, É., M. Basseville, F. Bourquin, L. Mevel, H. Nasser, and F. Treyssède. 2008. “Merging sensor data from multiple temperature scenarios for vibration-based monitoring of civil structures,” *Struct. Health Monit.*, 7(2):129-142.
4. Lu Y., Ye L. Su Z.: Crack identification in aluminium plates using Lamb wave signals of a PZT sensor network, *Smart Materials and Structures* 15: 839–849, 2006.
5. Wandowski T., Malinowski P., Ostachowicz W.: Geometrical approach to damage localization in panels, *Proc. of the 4th European Workshop on Structural Health Monitoring*, , pp. 784–791, Cracow, Poland, 2008.
6. Peeters B., Guillaume P., Van der Auweraer H., Cauberghe B., Verboven P., Leuridan J., Automotive and aerospace applications of the LMS PolyMAX modal parameter estimation method, *IMAC 22*, Dearborn (MI), USA, 2004.
7. B. Peeters, L. Mevel, S. Vanlanduit, P. Guillaume, M. Goursat, A. Vecchio, H. Van der Auweraer “Online Vibration-based Crack Detection During Fatigue Testing” *Key Engineering Materials Vols. 245-246 (2003) pp. 571-578*



#### CONTRIBUTING AUTHOR COPYRIGHT RELEASE FORM

As author of the chapter/contribution titled: **Comparison of the three different approaches for damage detection in the part of the composite wind turbine blade**

to appear in the *Proceedings of Structural Health Monitoring 2007*, I hereby agree to the following:

1. To grant to DEStech Publications, Inc., 1148 Elizabeth Avenue #2, Lancaster, PA, 17601, copyright of the above named chapter/contribution (for U.S. Government employees to the extent transferable), in print, electronic, and online formats. However, the undersigned reserve the following:
  - a. All proprietary rights other than copyright, such as patent rights.
  - b. The right to use all or part of this article in future works.

DEStech Publications thereby retains full and exclusive right to publish, market, and sell this material in any and all editions, in the English language or otherwise.

2. I warrant to DEStech Publications, Inc., that I am the (an) author of the above-named chapter/contribution and that I am the (a) copyright holder of the above-named chapter/contribution granted to DEStech Publications, Inc.
3. I warrant that, where necessary and required, I have obtained written permission for the use of any and all copyrighted materials used in the above-named chapter/contribution. I understand that I am responsible for all costs of gaining written permission for use of copyrighted materials.
4. I agree to assume full liability to DEStech Publications, Inc. and its licensee, and to hold DEStech Publications, Inc. harmless for any claim or suit filed against DEStech Publications, Inc. for violation of copyrighted material used in the above-named contribution.

Please sign and date this form and retain a copy for your records. Please include original form with your chapter/paper.

Thank you for your cooperation.

Please print name: Marcin Luczak

Signed:  Dated: 28.05.2009

1148 ELIZABETH AVENUE #2 • LANCASTER, PENNSYLVANIA 17601-4359, U.S.A.  
Toll Free: (866) 401-4337 • Tel: (717) 290-1660 • Fax: (717) 509-6100  
E-mail: [info@destechpub.com](mailto:info@destechpub.com) • Internet address: [www.destechpub.com](http://www.destechpub.com)